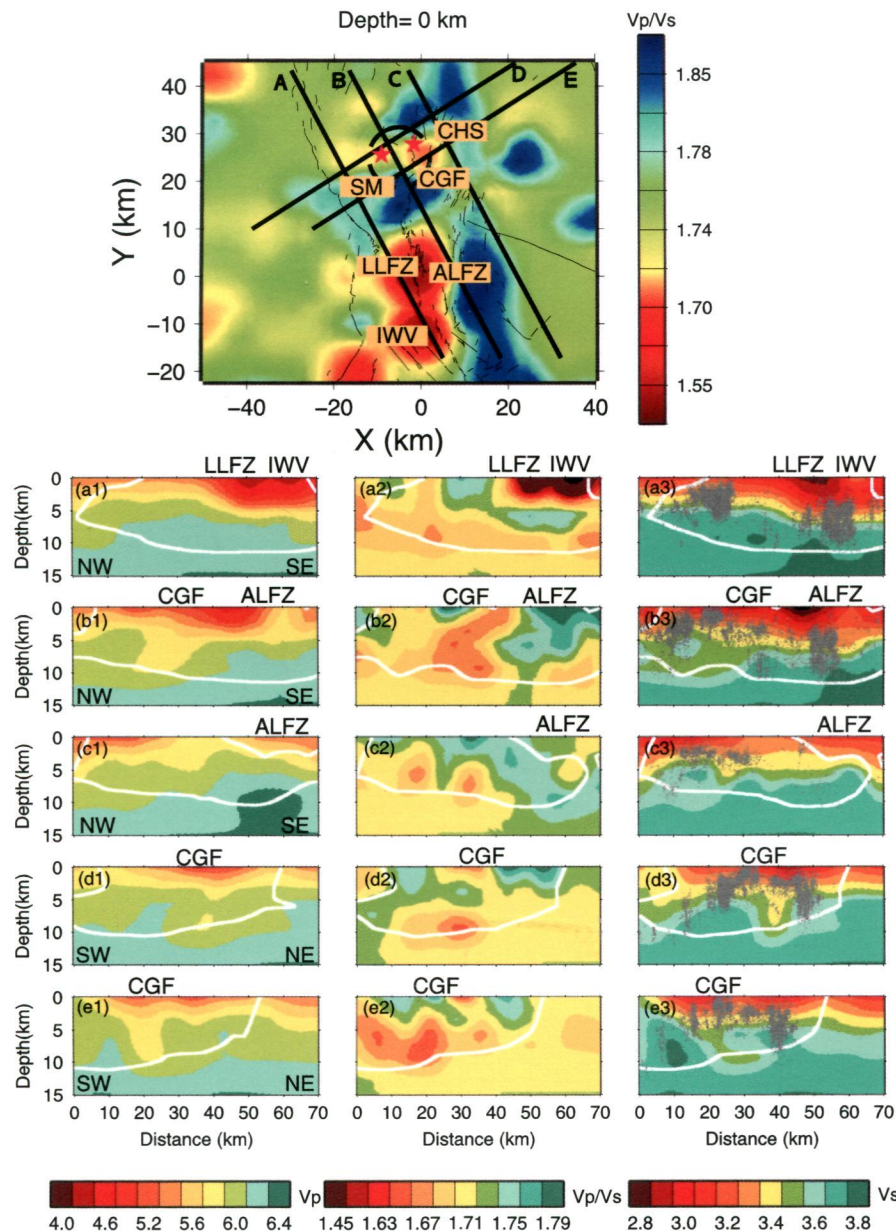


ПИ
У80/gr



Journal of Geophysical Research Solid Earth

Volume 119 Issue 6 June 2014
JGREA2(6) 4517–5274 (2014)
ISSN 2169-9313 (print); ISSN 2169-9356 (Online)

The online article is the official version and may contain additional content not available in this print issue. To access the full article, including multimedia, enhanced figures, supporting information, and other nonprinted content, go to <http://wileyonlinelibrary.com/journal/jgrb>.

Geomagnetism and Paleomagnetism/Marine Geology and Geophysics

- 4517** *Yang Zha, Spahr C. Webb, Scott. L. Nooner, and Wayne C. Crawford*
Spatial distribution and temporal evolution of crustal melt distribution beneath the East Pacific Rise at 9°–10°N inferred from 3-D seafloor compliance modeling (doi 10.1002/2014JB011131)
- 4538** *Daniel S. Zimmerman, Santiago Andrés Triana, Henri-Claude Nataf, and Daniel P. Lathrop*
A turbulent, highmagnetic Reynolds number experimental model of Earth's core (doi 10.1002/2013JB010733)

Chemistry and Physics of Minerals and Rocks/Volcanology

- 4558** *S. Alevizos, T. Poulet, and E. Veveakis*
Thermo-poro-mechanics of chemically active creeping faults. 1: Theory and steady state considerations*
(doi 10.1002/2013JB010070)
***Companion to Veveakis et al. [2014], doi:10.1002/2013JB010071, and Poulet et al. [2014], doi:10.1002/2014JB011004. doi:10.1002/2013JB010070**
- 4583** *E. Veveakis, T. Poulet, and S. Alevizos*
Thermo-poro-mechanics of chemically active creeping faults: 2. Transient considerations* (doi 10.1002/2013JB010071)
***Companion to Alevizos et al. [2014], doi:10.1002/2013JB010070, and Poulet et al. [2014], doi:10.1002/2014JB011004**
- 4606** *T. Poulet, E. Veveakis, K. Regenauer-Lieb, and D. A. Yuen*
Thermo-poro-mechanics of chemically active creeping faults: 3. The role of serpentinite in episodic tremor and slip sequences, and transition to chaos* (doi 10.1002/2014JB011004)
***Companion to Alevizos et al. [2014], doi:10.1002/2013JB010070, and Veveakis et al. [2014], doi:10.1002/2013JB010071**
- 4626** *J. Gottsmann and H. Odbert*
The effects of thermomechanical heterogeneities in island arc crust on time-dependent preeruptive stresses and the failure of an andesitic reservoir (doi 10.1002/2014JB011079)
- *This article is part of a Special Section—Stress, Strain and Mass Changes at Volcanoes**
- 4640** *Elodie Amiguet, Bertrand Van De Moortèle, Patrick Cordier, Nadège Hilairet, and Bruno Reynard*
Deformation mechanisms and rheology of serpentines in experiments and in nature (doi 10.1002/2013JB010791)
- 4656** *K. Ohta, K. Fujino, Y. Kuwayama, T. Kondo, K. Shimizu, and Y. Ohishi*
Highly conductive iron-rich (Mg,Fe)O magnesiowüstite and its stability in the Earth's lower mantle
(doi 10.1002/2014JB010972)
- 4666** *Thomas Reverso, Jean Vandemeulebrouck, François Jouanne, Virginie Pinel, Thierry Villemin, Erik Sturkell, and Pascale Bascou*
A two-magma chamber model as a source of deformation at Grímsvötn Volcano, Iceland (doi 10.1002/2013JB010569)
- 4684** *Shigehiko Tateno, Kei Hirose, and Yasuo Ohishi*
Melting experiments on peridotite to lowermost mantle conditions (doi 10.1002/2013JB010616)
- 4695** *S. Pinkert and J. L. H. Grozic*
Prediction of the mechanical response of hydrate-bearing sands (doi 10.1002/2013JB010920)
- 4708** *O. Galland, G. R. Gisler, and Ø. T. Haug*
Morphology and dynamics of explosive vents through cohesive rock formations (doi 10.1002/2014JB011050)

Seismology

- 4729** *Kaoru Sawazaki and Bogdan Enescu*
Imaging the high-frequency energy radiation process of a main shock and its early aftershock sequence: The case of the 2008 Iwate-Miyagi Nairiku earthquake, Japan (doi 10.1002/2013JB010539)
- 4747** *Tom Richter, Christoph Sens-Schönfelder, Rainer Kind, and Günter Asch*
Comprehensive observation and modeling of earthquake and temperature-related seismic velocity changes in northern Chile with passive image interferometry (doi 10.1002/2013JB010695)
- 4766** *Tao Wang, Justin Revenaugh, and Xiaodong Song*
Two-dimensional/three-dimensional waveform modeling of subducting slab and transition zone beneath Northeast Asia (doi 10.1002/2014JB011058)
- 4787** *Ryoko Nakata, Mamoru Hyodo, and Takane Hori*
Possible slip history scenarios for the Hyuga-nada region and Bungo Channel and their relationship with Nankai earthquakes in southwest Japan based on numerical simulations (doi 10.1002/2014JB010942)
- 4802** *C. P. Legendre, F. Deschamps, L. Zhao, S. Lebedev, and Q.-F. Chen*
Anisotropic Rayleigh wave phase velocity maps of eastern China (doi 10.1002/2013JB010781)
- 4821** *Bryan M. Kaproth and Chris Marone*
Evolution of elastic wave speed during shear-induced damage and healing within laboratory fault zones (doi 10.1002/2014JB011051)
- 4841** *A. E. Elbanna and J. M. Carlson*
A two-scale model for sheared fault gouge: Competition between macroscopic disorder and local viscoplasticity (doi 10.1002/2014JB011001)
- 4860** *M. Bernauer, A. Fichtner, and H. Igel*
Reducing nonuniqueness in finite source inversion using rotational ground motions (doi 10.1002/2014JB011042)
- 4876** *Tex Kubacki, Keith D. Koper, Kristine L. Pankow, and Michael K. McCarter*
Changes in mining-induced seismicity before and after the 2007 Crandall Canyon Mine collapse (doi 10.1002/2014JB011037)
- 4890** *Yan Wu and Xiaofei Chen*
The scale-dependent slip pattern for a uniform fault model obeying the rate- and state-dependent friction law (doi 10.1002/2013JB010779)
- 4907** *Qiong Zhang and Guoqing Lin*
Three-dimensional Vp and Vp/Vs models in the Coso geothermal area, California: Seismic characterization of the magmatic system (doi 10.1002/2014JB010992)
- 4923** *Garrett Ito, Robert Dunn, Aibing Li, Cecily J. Wolfe, Alejandro Gallego, and Yuanyuan Fu*
Seismic anisotropy and shear wave splitting associated with mantle plume-plate interaction (doi 10.1002/2013JB010735)
- 4938** *Ekaterina Kasatkina, Ivan Koulakov, Michael West, and Pavel Izbekov*
Seismic structure changes beneath Redoubt Volcano during the 2009 eruption inferred from local earthquake tomography (doi 10.1002/2013JB010935)
- 4955** *Vanessa M. King, Lisa V. Block, William L. Yeck, Christopher K. Wood, and Sarah A. Derouin*
Geological structure of the Paradox Valley Region, Colorado, and relationship to seismicity induced by deep well injection (doi 10.1002/2013JB010651)
- 4979** *Katrin Hannemann, Costas Papazachos, Matthias Ohrnberger, Alexandros Savvaidis, Marios Anthymidis, and Agostini M. Lontsi*
Three-dimensional shallow structure from high-frequency ambient noise tomography: New results for the Mygdonia basin-Euroseistest area, northern Greece (doi 10.1002/2013JB010914)
- 5000** *John G. Armbruster, Won-Young Kim, and Allan M. Rubin*
Accurate tremor locations from coherent S and P waves (doi 10.1002/2014JB011133)

Geodesy and Gravity/Tectonophysics

- 5014** *Ryan D. Gold, Richard W. Briggs, Stephen F. Personius, Anthony J. Crone, Shannon A. Mahan, and Stephen J. Angster*
Latest Quaternary paleoseismology and evidence of distributed dextral shear along the Mohawk Valley fault zone, northern Walker Lane, California (doi 10.1002/2014JB010987)
- 5033** *S. Sainz-Maza Aparicio, J. Arnoso Sampedro, F. Gonzalez Montesinos, and J. Martí Molist*
Volcanic signatures in time gravity variations during the volcanic unrest on El Hierro (Canary Islands) (doi 10.1002/2013JB010795)
- 5052** *Zhong-Hai Li, Jeanette F. Di Leo, and Neil M. Ribe*
Subduction-induced mantle flow, finite strain, and seismic anisotropy: Numerical modeling (doi 10.1002/2014JB010996)

- 5077** *David M. Whipp Jr., Christopher Beaumont, and Jean Braun*
Feeding the “aneurysm”: Orogen-parallel mass transport into Nanga Parbat and the western Himalayan syntaxis
(doi 10.1002/2013JB010929)
- 5097** *K. Chanard, J. P. Avouac, G. Ramillien, and J. Gernich*
Modeling deformation induced by seasonal variations of continental water in the Himalaya region: Sensitivity to Earth elastic structure (doi 10.1002/2013JB010451)
- 5114** *Marion Y. Thomas, Jean-Philippe Avouac, Johann Champenois, Jian-Cheng Lee, and Long-Chen Kuo*
Spatiotemporal evolution of seismic and aseismic slip on the Longitudinal Valley Fault, Taiwan
(doi 10.1002/2013JB010603)
- 5140** *Bryan Riel, Mark Simons, Piyush Agram, and Zhongwhen Zhan*
Detecting transient signals in geodetic time series using sparse estimation techniques (doi 10.1002/2014JB011077)
- 5161** *D. S. Stamps, L. M. Flesch, E. Calais, and A. Ghosh*
Current kinematics and dynamics of Africa and the East African Rift System (doi 10.1002/2013JB010717)
- 5187** *J. F. Kirby and C. J. Swain*
The long-wavelength admittance and effective elastic thickness of the Canadian Shield (doi 10.1002/2013JB010578)
- 5215** *R. J. Walters, B. Parsons, and T. J. Wright*
Constraining crustal velocity fields with InSAR for Eastern Turkey: Limits to the block-like behavior of Eastern Anatolia
(doi 10.1002/2013JB010909)
- 5235** *William C. Hammond, Geoffrey Blewitt, and Corné Kreemer*
Steady contemporary deformation of the central Basin and Range Province, western United States
(doi 10.1002/2014JB011145)
- 5254** *Andrew J. Barbour and Frank K. Wyatt*
Modeling strain and pore pressure associated with fluid extraction: The Pathfinder Ranch experiment
(doi 10.1002/2014JB011169)

Cover. Cross sections of the V_p, V_p/V_s, and V_s structures across and in proximity to the CGF. The geothermal field is denoted by the dashed circle with the red stars marking the locations of the SM and CHS. The five profiles are shown by the black lines with profiles B, D, and E passing through the geothermal field and A and C off the CGF. Relocated earthquakes within 5 km of both sides of the profiles are projected to the V_s cross sections, denoted by grey dots. White contour lines represent the RDE values greater than 0.1. See *Zhang and Lin*, pp. 4907–4922, doi: 10.1002/2014JB010992.